

## Box-Behnken Experimental Design for Electrochemical Aptasensor Optimization on Screen Printed Carbon Electrode/Silica-Ceria

Salma Nur Zakiyyah<sup>1</sup>, Diana Rakhmawaty Eddy<sup>1</sup>, Muhammad Lutfi Firdaus<sup>2</sup>, Toto Subroto<sup>3</sup>, Yeni Wahyuni Hartati<sup>1\*</sup>

<sup>1</sup>Department of Chemistry, Faculty of Mathematics and Sciences, Universitas Padjadjaran  
Jl. Raya Bandung-Sumedang km. 21 Jatinangor, Sumedang 45363, Indonesia

<sup>2</sup>Graduate School of Science Education, Bengkulu University

Jl. W.R. Supratman Kandang Limun, Bengkulu 38371, Indonesia

<sup>3</sup>Bionformatics and Biomolecular Research Center, Universitas Padjadjaran  
Jl. Singaperbangsa 2, Bandung 40132, Indonesia

\*Corresponding author: [yeni.w.hartati@unpad.ac.id](mailto:yeni.w.hartati@unpad.ac.id)

Received: August 2022; Revision: November 2022; Accepted: April 2023; Available online: May 2023

### Abstract

This study aims to optimize the epithelial sodium channel (ENaC) electrochemical aptasensor with the Box-Behnken experimental design. ENaC is a protein that plays a role in sodium ion transport in several epithelial tissues and is associated with hypertension. The ENaC protein aptamer is held in place in the electrochemical aptasensor by a modified screen-printed carbon electrode (SPCE) of silica-ceria composite (SiO<sub>2</sub>-CeO<sub>2</sub>). The unique structure of a silica matrix with high biocompatibility can form composites through a hydrothermal process. The Box-Behnken design is an efficient optimization method of factors that affect the experiment at three levels. The FTIR results of the silica-ceria composites were 549.35 cm<sup>-1</sup> (Ce-O), 1095.3 cm<sup>-1</sup> (Si-O-Si), and 491.28 cm<sup>-1</sup> (Si-O). Meanwhile, SPCE/silica-ceria characterized by differential pulse voltammetry (DPV) showed an increase in peak current [Fe(CN)<sub>6</sub>]<sup>3-/4-</sup> from 3.190 μA to 9.073 μA. Three experimental factors, aptamer concentration, streptavidin incubation time, and aptamer incubation time, were optimized with BBD and obtained at 0.5 μg.mL<sup>-1</sup>, 30 minutes, and 1 hour. The optimum conditions observed resulted in a selective current response for ENaC protein detection. The optimization results can be applied to aptamer-based ENaC protein detection in samples.

**Keywords:** Box-Behnken; electrochemical aptasensor; optimization; silica-ceria composite.

**DOI:** 10.15408/jkv.v9i1.27493

### 1. INTRODUCTION

The epithelial sodium channel (ENaC) is a major salt and water reabsorption regulator in several epithelial tissues. ENaC dysfunction is directly associated with several hypertension conditions (Choi et al., 2014). Epithelial sodium channels (ENaC) control the rate of sodium reabsorption by epithelial cells, which line the distal renal tubules, distal colon, ducts of several exocrine glands, and the lungs. ENaC resides on the apical membrane of cells in the distal nephron and is responsible for controlling Na<sup>+</sup> reabsorption. ENaC dysregulation is implicated in several conditions, including pulmonary edema, acute respiratory distress syndrome, nephrosis, and salt-dependent hypertension (Xu et al., 2016).

The level of salt intake can affect the biomarker ENaC protein, which indicates hypertension. To date, it has been proven that ENaC expression promotes Na<sup>+</sup> retention, which causes an increase in blood pressure (Reus-Chavarría et al., 2019). The urine sample is used because it is the closest source, namely the kidneys, which control blood pressure and ENaC (Sofiati & Roesli, 2018).

The ENaC protein detection method is a commonly used ELISA method, but it has drawbacks such as complex, time-consuming, and expensive procedures (Sakamoto et al., 2018). Other methods reported to detect ENaC are optical biosensors (García-Rubio et al., 2020), electrochemical biosensors such as immunosensors which have low levels of ENaC detection (Hartati et al., 2020), aptasensor

(Zakiyyah et al., 2022; Sari et al., 2022; Hartati et al., 2021; Fazrin et al., 2022; Khan et al., 2017; Khan et al., 2016). The advantages of the aptasensor are that it has high affinity, lower cost, and is easier to modify (Tan et al., 2019).

The use of SPCE in electrochemical sensors for ENaC has been reported to modify AuNP (Hartati et al., 2020; Hartati et al., 2021), and CeO<sub>2</sub> (Hartati et al., 2021). The choice of nanomaterials to modify the electrode aims to increase conductivity, compatibility, sensitivity, and performance. In this study, we developed an SPCE modification with silica-ceria nanocomposites.

Silicon dioxide (SiO<sub>2</sub>), also known as silica, is one example of a mineral in a natural resource that has the potential to be developed. Silica can be obtained through synthesis or extraction from natural materials. Natural resources in Indonesia are abundant and widely available, but still not utilized by human resources. Beaches in Indonesia are wide; one of them is in Bengkulu Province, which has beach sand with a high content of silica minerals (55.30–99.87% by weight). Therefore, silica from Bengkulu sand extraction (Ishmah et al., 2020) can reduce the use of hazardous materials and treatments that can reduce waste. Silica can be obtained from various sources but is mixed with other oxides and minerals, so separation is required to obtain pure silica using the alkaline fusion method (Firdaus et al., 2020). Silica nanoparticles have been reported for dopamine detection in biosensors with excellent performance and low detection limits (De Morais et al., 2012). Silica composites are used in electrochemical sensors because they have a large surface area and are stable (Ismail et al., 2020). Silica nanoparticles can be composited with metal nanoparticles. Silica-modified electrodes developed silica-Au nanocomposites for glucose oxidase enzymes detection (Bai et al., 2007), c-creative protein detection (Wang et al., 2017), and arsenic detection (Ismail et al., 2020). Biologically modified silica composites, in mono- or multilayer configurations, have been successfully applied in electroanalysis, especially biosensors (Walcarius, 2018).

Cerium oxide nanoparticles (CeO<sub>2</sub>), or ceria, are a transition metal oxide element with good potential in biosensors developed with high electron mobility. The advantages of ceria are its oxygen storage capacity in its structure, redox transition ability, enhanced electron transfer, biocompatibility, and high

conductivity. It improves sensitivity, selectivity, stability, and long-term bioactivity (Siangproh et al., 2011). The unique structure of a silica matrix with high biocompatibility can form a composite. The silica-ceria composite is an interesting material because silica can improve thermal stability. The hydrothermal method is a common method for the synthesis of silica-ceria composites (Li et al., 2009). Composites consist of two or more materials with different properties, with the constituent properties still present in the resulting material (Maharani & Hidayah, 2015).

The experimental design aims to determine the optimum conditions for the experimental factors with a significant effect. Optimization can use the Response Surface Methodology (RSM). RSM is a collection of statistical and mathematical techniques useful for development, improvement, and process optimization, where the response is influenced by several factors, resulting in a mathematical model that describes chemical or biochemical processes. RSM has the advantage of not requiring large amounts of experimental data and minimizing the short trial time (Radojković et al., 2012). The RSM method consists of two types of experimental designs: central composite design (CCD) and Box-Behnken design (BBD). In this study, the BBD was chosen because it has the advantage of a simple and efficient design with a small number of trials (3–4 factors) (Perincek & Colak, 2013). BBD uses three levels, namely high level (+), middle level (0), and low level (-). Then, response data is processed under optimal conditions, and factors are obtained (Wyantuti et al., 2021).

Biosensors based on an aptamer as an identifying element are referred to as aptasensors. Streptavidin can bind to the biotinylated aptamer, as reported in several aptasensor studies (Dundas et al., 2013). Streptavidin is a biotin-binding tetrameric protein isolated from *Streptomyces avidinii* (Sedlak et al., 2020). Streptavidin has four identical subunits, each of which can bind biotin with high affinity and specificity. The interaction that occurs between streptavidin-biotin is a non-covalent bond by biotin that binds to the tryptophan amino acid in the subunit. Biotinylation is the process of attaching biotin to proteins, nucleic acids, or other molecules (Chivers et al., 2011). This article will discuss chemical analysis carried out with

chemical sensors or biosensors with aspects of sustainability as green chemistry by paying attention to using samples and reagents, carrying out analyses in a shorter, simpler, and faster way. Biosensors with the advantage of minimizing the use of the equipment and conducting analysis on-site, outside the laboratory, or at the point of care (del Valle, 2021).

In realizing green chemistry, there is a role for biosensors. Currently, electrochemical sensors are widely recognized as sensitive detection tools for disease diagnosis and the detection of various species of pharmaceutical, clinical, industrial, food, and environmental origin. Electrochemical sensors can utilize materia that are biodegradable and sustainable. Biosensors can minimize the use of toxic or hazardous reagents and solvent systems, thereby further reducing the production of chemical waste in sensor fabrication. Paper-based SPCE is a naturally harmless material and the electrochemical performance of the biosensor has the benefits of biodegradability, non-toxicity, sustainability, low cost, and a sensitive surface (Kalambate et al., 2020). This article discusses the synthesis of ceria and silica-ceramic composites and their characterization, the modification of SPCE with composites and aptamer immobilization, the detection of ENaC protein, and optimization with the Box-Behnken method. The purpose of this article is to develop an electrochemical aptasensor optimization at the SPCE/Silika-Ceria electrode with the Box-Behnken method of experimental design.

## 2. MATERIALS AND METHODS

### Material and Tool

The materials used in this study were Silica nanoparticles (Ishmah et al., 2020), potassium chloride (KCl) (Merck), sodium hydroxide (NaOH) (Merck), bovine serum albumin (BSA) (Sigma Aldrich), ethanol (Merck), methanol (Merck), cerium nitrate ( $\text{Ce}(\text{NO}_3)_3 \cdot 6\text{H}_2\text{O}$ ) (Merck), biotin-conjugated aptamer (biotin 5'- CGG TGA GGG TCG GGT CCA GTA GGC CTA CTG TTG AGT AGT GGG CTC C -3') (Abcam), ENaC protein (PT. Elo Karsa Utama), aqua pro injection (PT. Ikapharmindo Putramas), streptavidin (Promega), phosphate buffered saline (PBS) pH 7.4 (VWR), and solid potassium ferricyanide  $\text{K}_3[\text{Fe}(\text{CN})_6]$  (Sigma Aldrich).

The tools used in this study were screen-printed carbon electrode (SPCE) (GSI Technologies, USA), potentiostat (Zimmer and Peacock), fourier transform infra-red (FT-IR) spectrometer (Thermo Scientific), scanning electron microscopy (SEM) (Hitachi TM3000), particle size analyzer (PSA) (Horiba SZ-100), and UV-Vis spectrophotometer (Thermo Scientific G10S UV-Vis).

### Preparation of Ceria Nanoparticles

Two g of cerium nitrate hexahydrate ( $\text{Ce}(\text{NO}_3)_3 \cdot 6\text{H}_2\text{O}$ ) was dissolved in 50 mL of aqua pro injection. Then, the solution was stirred and 25 mL of 0.1 M NaOH was dripped with constant stirring for 30 minutes at room temperature. After that, the mixture was allowed to stand for 1 hour until a pale yellowish-white precipitate was obtained. The mixture was centrifuged at 8000 rpm for 20 minutes. Then, the precipitate was washed several times, dried at 70 °C for 2 hours, and cooled to room temperature. Then, the solid was calcined overnight at 240 °C to obtain a powder of ceria nanoparticles. Solids were characterized by UV-Vis spectrophotometer and PSA (Ali et al., 2018).

### Preparation of Composite

Silica resulting from extraction carried out by (Ishmah et al., 2020) was added to a mixture of 4.5 mL of distilled water and 14.5 mL of absolute ethyl alcohol, then sonicated for 15 minutes. The mixture was sequentially added 0.018 g silica for 3 minutes, 0.1031 g  $\text{CeO}_2$  for 45 minutes, and 10 mL aqua pro injection for 20 minutes in a sonicator, then the mixture was cooled at room temperature. The mixture was centrifuged at 6000 rpm for 10 minutes to form a composite  $\text{CeO}_2\text{-SiO}_2$  precipitate. The precipitate was dried at 110 °C for 2 hours, and the solid was calcined at 500 °C for 5 hours. Then, the solid is dispersed in 50 mL of methanol. Solids were characterized by UV-Vis spectrophotometer and FTIR (Phanichphant et al., 2016).

### Modified of SPCE/Silica-Ceria Composite

SPCE was washed to remove dirt on the surface of SPCE with aqua pro injection two times, and then SPCE was dried at room temperature (Ismail et al., 2020b). The composite solution was dripped onto the SPCE surface and left to dry. Then the SPCE was rinsed with aqua pro injection, and the SPCE

was left to dry. SPCE was characterized using voltammetry with the differential pulse voltammetry (DPV) method in 10 mM  $K_3[Fe(CN)_6]$  containing 0.1 M KCl as a supporting electrolyte at a potential range of -1.0 to 1.0 V with a scan rate of 0.008 V/s and characterized by energy-dispersive X-ray spectroscopy (EDS) (Bai et al., 2007).

### Immobilization of Biomolecules on SPCE/Silica-Ceria

SPCE was dripped with 50  $\mu\text{g/mL}$  streptavidin on its clean surface and incubated in the refrigerator, then rinsed and dried. SPCE was added with 0.5  $\mu\text{g/mL}$  aptamer-biotin, as much as 10  $\mu\text{L}$ . SPCE was incubated, rinsed, and dried. SPCE was added to 15  $\mu\text{L}$  of 1% BSA for 20 minutes and then rinsed. Next, SPCE was dripped with 15  $\mu\text{L}$  of ENaC protein and SPCE was incubated for 20 minutes, rinsed, and dried. SPCE was characterized using DPV in 10 mM  $K_3[Fe(CN)_6]$  containing 0.1 M KCl as a supporting electrolyte over a potential range of -1.0 to 1.0 V at a scan rate of 0.008 V/s and characterized by EDS (Bai et al., 2007).

### Parameter Optimization

Optimizing the parameters that affect the experiment, the parameters used are ENaC aptamer concentration (X1), streptavidin protein incubation time (X2), and ENaC aptamer incubation time (X3). Factors are designed at 3 different levels in **Table 1**.

**Table 1** Factor and level of analysis of optimization of experimental conditions

Factor	Unit	Level		
		-1	0	+1
ENaC aptamer concentration (X1)	$\mu\text{L/mL}$	0.5	1	1.5
Streptavidin protein incubation time (X2)	Minutes	30	60	90
ENaC aptamer incubation time (X3)	Hours	1	2	16

## 3. RESULTS AND DISCUSSION

Various methods, including the simple precipitation method, can synthesize ceria nanoparticles. The precipitation method is one of the most promising techniques due to its inexpensive starting materials, simple synthesis processes with reproducible results, and commonly available equipment. Factors that affect the synthesis with the precipitation

method are temperature and time of calcination, addition, type of surfactant, and temperature during synthesis (Jalilpour & Fathalilou, 2012). The ceria particle synthesis used cerium (III) nitrate hexahydrate and sodium hydroxide as precipitants (Fadzil et al., 2018). The results of the UV-Vis spectrophotometric characterization of the ceria particles show absorbance peaks at 308 nm (**Figure 1a**). The maximum wavelength is generally 250–400 nm (Pujar et al., 2018). The PSA characterization is used to determine the size of the ceria particles in dispersions using the dynamic light scattering method. The PSA results in **Table 2** show that the size of the ceria particles formed is 251.6 nm. The polydispersity index (PI) value describes the width or narrowness of a particle size distribution. The higher the PI value, the more unstable the nanoparticles are. If the PI value is  $> 0.7$ , it has a wide distribution of particle sizes which causes low stability, making it easy to agglomerate quickly (Danaei et al., 2018). The PSA results found that the PI value was 0.3, so this synthesis result was quite stable.

**Table 2.** The result data of particle ceria characterized using PSA.

Histogram Operations	Size (nm)
Size (Median)	251.6
Size (Average)	288.2
PI	0.379

### Characterization of Silica Nanoparticles

The UV-Vis spectrophotometric characterization results of silica nanoparticles have a peak at 300 nm, as shown in Figure 1b. Based on the data that the peaks of silica nanoparticles are at wavelengths around 200–800 nm, and particle size can also affect the absorption wavelength (Intartaglia et al., 2012). Then, PSA characterization was also carried out to determine the size of the silica nanoparticles formed. The PSA results in **Table 3** show that the silica particles formed are 99.7 nm in size. A particle can be a nanoparticle if it has a particle size  $< 100$  nm (Vert et al., 2012), so the silica used is nanoparticle size. The result of the PI value was known to be 0.3, so the silica nanoparticles obtained were stable because the PI value  $< 7$ .

**Table 3** The result data of particle ceria characterized using PSA.

Histogram Operations	Size (nm)
Size (Median)	99.7
Size (Average)	114.3
PI	0.395

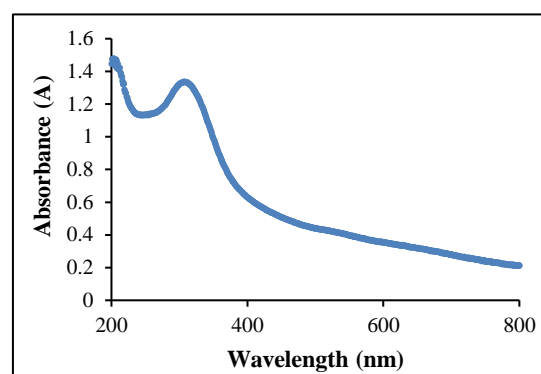
### Characterization of Silica-Ceria Nanocomposites

Preparation of composites for modifying the electrode. Silica-ceria nanocomposites with small crystal sizes and large surface areas can withstand even high-temperature conditions because the primary crystals offered are amorphous silica. In the formation of composites, silicon oxide acts as a source of silica and ceria as a precursor (Nguyen et al., 2019).

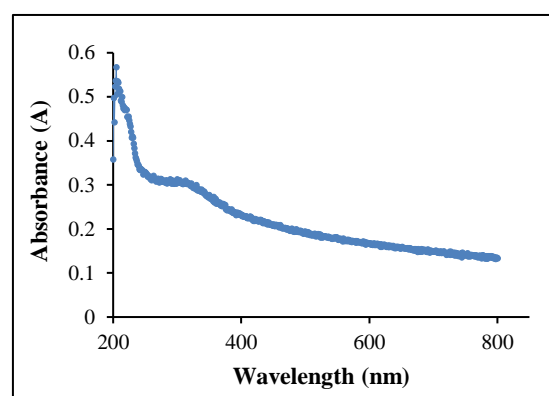
UV-Vis spectrophotometry results showed nanocomposite silica-ceria to have an absorption peak at 337 nm with a small peak at 231 nm (**Figure 1c**). The peaks at the maximum wavelength range for silica-ceria composites are in the range of 250–400 nm (Xunwen, 2020) and research has small shoulders around 200–300 nm (Dalmis et al., 2020).

The electrode was modified with a silica-ceria composite with a mole ratio of 1:2 due to optimal conditions in previous studies (Xunwen et al., 2020). In **Figure 2**, silica particles have a smooth surface and are negatively charged in neutral or alkaline dispersions. When  $\text{Ce}(\text{NO}_3)_3 \cdot 6\text{H}_2\text{O}$  is added, positively charged  $\text{Ce}^{3+}$  ions are attracted to the surface of  $\text{SiO}_2$  via electrostatic interactions in a weakly basic environment.

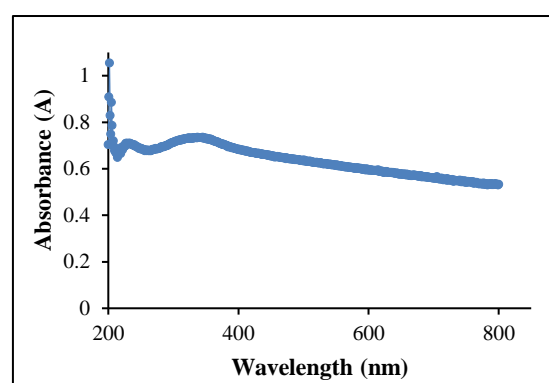
The results of FTIR characterization can be used to identify compounds, detect functional groups, and analyze mixtures of the samples. In **Figure 3**, the peaks are obtained at frequencies of  $3440.9 \text{ cm}^{-1}$  (O-H stretching),  $2015.22 \text{ cm}^{-1}$  (C-H),  $549.35 \text{ cm}^{-1}$  (Ce-O),  $1621.51 \text{ cm}^{-1}$  (O-H bonding),  $1095.3 \text{ cm}^{-1}$  (Si-O-Si), and  $491.28 \text{ cm}^{-1}$  (Si-O). Based on Ishmah et al. (2020) and Calvache-Muñoz et al. (2017). The FTIR results of this study indicate that the procedure can form composites.



(a)



(b)



(c)

**Figure 1.** The results of characterization using a UV-Vis spectrophotometer a) Ceria particles have a maximum wavelength of 308 nm b) Silica nanoparticles have a wavelength of 300 nm c) Silica-Ceria composite has a maximum wavelength of 337 nm with a small peak at 231 nm.

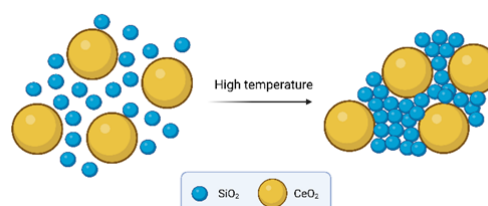


**Figure 2.** Schematic of the reaction silica-ceria composite adapted by Nguyen et al., 2019, created by biorender.com.

### SPCE/Composite Characterization

Electrode modifications are needed to increase the sensitivity to the required biosensor sensing. **Figure 4a** shows the peak current from the unmodified or bare SPCE and **Figure 4b** shows a significant increase in the current generated by the SPCE after being modified by the silica-ceria composite. The following is the ferri-ferrocyanide redox reaction at the electrode surface that occurs (Scholz, 2010):

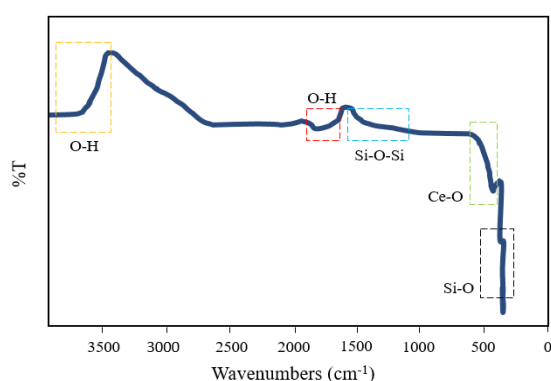
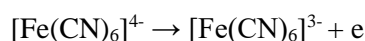
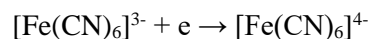


**Figure 3.** FTIR spectrum of silica-ceria nanocomposite.

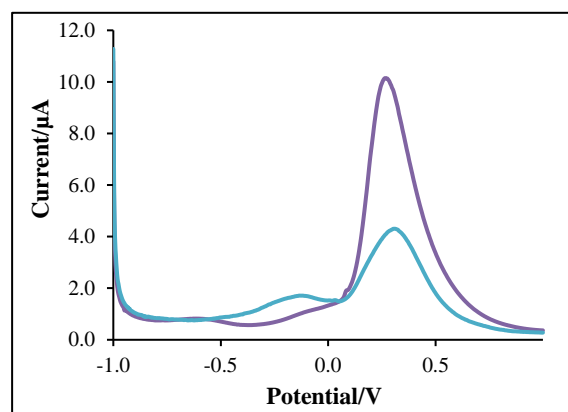


**Figure 4.** DPV characterization results from SPCE before and after composite modification. a) bare SPCE and b) SPCE/composite.

### Characterization of Biomolecule Immobilized on SPCE/Composites

In modifying the electrodes, biomolecules used that function so that specific bonds occurred in biosensor analysis. The use of biomolecules in biosensors, especially electrochemistry, is growing because it is important and needed, namely for detecting low and fast but simple limits. Immobilising the

streptavidin biomolecule on the electrode surface can bind specifically to the previously designed ENaC aptamer (Komala et al., 2021) with a biotin end. The interaction is one of the strongest non-covalent interactions in nature because it has a high affinity between streptavidin and biotin. The interactions are hydrogen bonds and van der Waals forces, which are hydrophobic. The streptavidin-biotin interaction also binds like an antibody to an antigen, namely lock and key (Chivers et al., 2011).

On the composite, when streptavidin protein is added, adsorption occurs due to electrostatic, hydrophobic, and physical adsorption interactions. Some factors influence the condition of the atmosphere's pH and concentration (Hyre, 2006). Ceria in the silica-ceria composite strongly interacts with the  $-\text{NH}_2$  group to bind streptavidin and thionine for matrix metalloproteinase 2 biosensors, and ceria can form bridge bonds with the carboxyl functional groups of antibodies even without the addition of other agents (Hartati et al., 2021). The amphipathic structure of proteins can be nonspecifically bound to the silica surface due to the curvature of the silica and molecular weight, the constant affinity of the protein, and the adsorption process (Ma et al., 2015).

**Figure 5** shows the characterization results using DPV on SPCE with modified composites and biomolecules. The peak DPV currents of (5a) SPCE/composite, (5b) bare SPCE, (5c) SPCE/composite/streptavidin, (5d) SPCE/composite/streptavidin/aptamer, and (5e) SPCE/composite/streptavidin/aptamer/ENaC, respectively 9, 3, 9, 3, 2, and 1 A shows a decrease in current after the addition of biomolecules. Biomolecules are non-conductive large molecules, so they can inhibit electron transfer, which results in a decrease in the peak current from  $\text{K}_3[\text{Fe}(\text{CN})_6]$ . (Hartati et al., 2021).

In **Table 4**, the EDS characterization result shows four elements contained in the modified SPCE composite, namely carbon, which is the content of the SPCE electrode used; oxygen; silicon; and cerium, which are present in the composite. So, the results indicate that SPCE modified the composite.

The EDS characterised the results for the SPCE-modified streptavidin biomolecules. **Table 5**, There are five elements, namely carbon, which is the content of the SPCE

electrode used; oxygen, silicon, and cerium, which are present in the composite; and nitrogen, which is the content present in the streptavidin protein. So, the results indicate that SPCE is immobilized streptavidin.

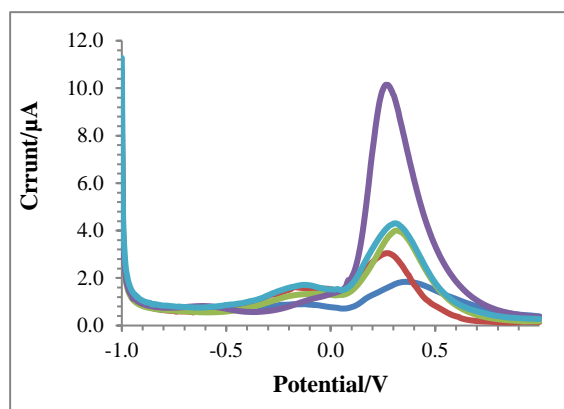


**Figure 5** DPV characterization results from a) SPCE/composite, b) bare SPCE, c) SPCE/composite/streptavidin, d) SPCE/composite/streptavidin/aptamer, e) SPCE/composite/streptavidin/aptamer/ENaC.

**Table 4.** EDS characterization results on SPCE/composite surfaces

Element	Weight %
Carbon	8.699
Oxygen	29.260
Silicon	7.024
Cerium	55.017

**Table 5.** EDS characterization results on SPCE/composite/streptavidin surfaces

Element	Weight %
Carbon	37.601
Oxygen	24.130
Silicon	2.275
Cerium	32.621
Nitrogen	3.372

### Determination of Optimum Conditions with The Box-Behnken Experimental Design

Optimization factors carried out in this study were aptamer concentration (X1), streptavidin incubation time (X2), and ENaC aptamer incubation time (X3). For each factor, the lowest and highest values were determined from previous experiments conducted by Hartati et al. (2020) regarding an immunosensor to detect the ENaC protein, which has been carried out with a well-designed range of values.

**Table 1** shows that each factor is designed through three levels, namely the lowest (-1), middle (0), and highest (+1) levels. The Box-Behnken design is arranged into three replication blocks for three repetitions so that the number of experiments becomes 45, with the response results in the form of a current response shown in **Table 6**.

The measurement results are processed using Minitab 19 with the ANOVA method, so the response is to obtain the optimum current. This method is a statistical analysis widely used in experimental research to find the optimal value of a response. Based on the results of the ANOVA analysis, the factors that significantly influenced the experiment had a P-value 0.05. **Table 6** shows the results of the responses of each factor carried out in the experiment. Based on the current response obtained, it is analysed to obtain the coefficient of the response function in **Equation 1**.

$$Y = -1.379 + 0.597 X_1 + 0.0688 X_2 + 0.484 X_3 + 0.004 X_1^2 - 0.000463 X_2^2 - 0.02091 X_3^2 - 0.00927 X_1 X_2 - 0.0459 X_1 X_3 - 0.000667 X_2 X_3 \dots (1)$$

Where X1 is ENaC aptamer concentration, X2 is Streptavidin protein incubation time, and X3 is ENaC aptamer incubation time.

Based on **Equation 1**, it shows that factors with negative values affect decreasing the response, while factors with positive values affect increasing the response in the experiment. In **Figure 6**, the results of the Box-Behnken design obtained optimum conditions for each factor, namely the ENaC aptamer concentration of  $0.5 \mu\text{g.mL}^{-1}$ , streptavidin protein incubation time of 30 minutes, and ENaC aptamer incubation time of 1 hour. Then, this optimum condition is used for every detection of the ENaC protein.

In **Table 7**, the optimization results obtained two factors that significantly influenced the study because the concentration factor of the ENaC aptamer and the incubation time factor of the ENaC aptamer had a P-value of less than 0.5. The lack of fit of the research obtained a P-value of 0.2047 or greater than 0.05, so it can be concluded that the resulting linear model is appropriate. Lack of fit indicates a deviation or inaccuracy of the linear model, so the tests aim to detect whether the linear model is appropriate (Jekel et al., 2018).

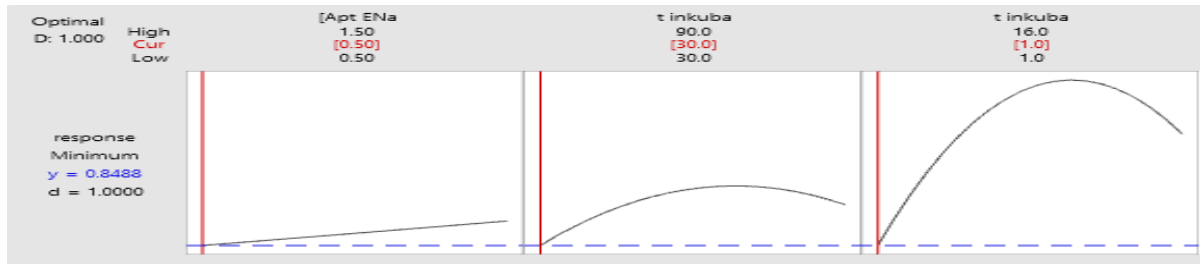


Figure 6. The graph of the aptasensor optimization results uses the Box-Behnken design

Table 6. Factor, level anlevel,rent response analysis optimization of experimental conditions

ENaC aptamer concentration ( $\mu\text{g.mL}^{-1}$ )	Streptavidin incubation time (Minute)	ENaC aptamer incubation time (Hours)	Response ( $\mu\text{A}$ )
0.5	30	2	1.124
1.5	30	2	1.618
0.5	90	2	1.289
1.5	90	2	1.493
0.5	60	1	1.378
1.5	60	1	1.116
0.5	60	16	2.704
1.5	60	16	1.673
1	30	1	1.150
1	90	1	1.124
1	30	16	2.416
1	90	16	1.211
1	60	2	1.352
1	60	2	1.531
1	60	2	1.742
0.5	30	2	1.262
1.5	30	2	1.359
0.5	90	2	1.078
1.5	90	2	1.191
0.5	60	1	1.42
1.5	60	1	1.325
0.5	60	16	2.396
1.5	60	16	2.326
1	30	1	1.312
1	90	1	1.103
1	30	16	1.625
1	90	16	1.634
1	60	2	1.776
1	60	2	1.842
1	60	2	1.666
0.5	30	2	1.105
1.5	30	2	1.208
0.5	90	2	2.82
1.5	90	2	1.528
0.5	60	1	1.278
1.5	60	1	1.670
0.5	60	16	2.795
1.5	60	16	1.842
1	30	1	1.292
1	90	1	1.373
1	30	16	1.369
1	90	16	1.297
1	60	2	2.119
1	60	2	2.328
1	60	2	2.193

**Table 7.** P value of ANOVA results for each factor

	P Value
ENaC aptamer concentration	0.0499
Streptavidin incubation time	0.5358
ENaC aptamer incubation time	0.0001
Lack of fit	0.2047

#### 4. CONCLUSIONS

The silica-ceria nanocomposite characterised by DPV shows an increase in the current peak  $[\text{Fe}(\text{CN})_6]^{3-/4-}$ . The streptavidin and biotin-aptamer biomolecules could be immobilised via non-covalent interaction on the electrode surface. The optimum conditions of the experiment were obtained through the Box-Behnken experimental design, namely aptamer concentration, streptavidin incubation time, and aptamer incubation times of  $0.5 \mu\text{g}\cdot\text{mL}^{-1}$ , 30 minutes, and 1 hour. This showed the development of a modified electrochemical aptasensor method with nanocomposites developed to detect ENaC as a hypertension biomarker. In green chemistry, the biosensor method could reduce reagents and samples as well as point of care. In addition, the chemometric method was applied to optimise the method. Using silica derived from natural materials is a good resource utilisation strategy and can continue to be a future development in biosensors.

#### ACKNOWLEDGMENTS

The support for this study was provided by Universitas Padjadjaran Academic Leadership Grant and BUPP Scheme No. 2203/UN6.3.1/PT.00/2022 and is gratefully acknowledged.

#### REFERENCES

- Ali, M. M., Mahdi, H. S., Parveen, A., & Azam, A. (2018). Optical properties of cerium oxide ( $\text{CeO}_2$ ) nanoparticles synthesized by hydroxide mediated method. *AIP Conference Proceedings*, 1953, 1–5. <https://doi.org/10.1063/1.5032379>
- Bai, Y., Yang, H., Yang, W., Li, Y., & Sun, C. (2007). Gold nanoparticles-mesoporous silica composite used as an enzyme immobilization matrix for amperometric glucose biosensor construction. *Sensors and Actuators, B: Chemical*, 124(1), 179–186. <https://doi.org/10.1016/j.snb.2006.12.020>
- Calvache-Muñoz, J., Prado, F. A., & Rodríguez-Páez, J. E. (2017). Cerium oxide nanoparticles: Synthesis, characterization and tentative mechanism of particle formation. *Colloids and Surfaces A: Physicochemical and Engineering Aspects*, 529, 146–159. <https://doi.org/10.1016/j.colsurfa.2017.05.059>
- Chivers, C. E., Koner, A. L., Lowe, E. D., & Howarth, M. (2011). How the biotin-streptavidin interaction was made even stronger: Investigation via crystallography and a chimaeric tetramer. *Biochemical Journal*, 435(1), 55–63. <https://doi.org/10.1042/BJ20101593>
- Choi, H. W., Lee, K. H., Hur, N. H., & Lim, H. B. (2014). Cerium oxide-deposited mesoporous silica nanoparticles for the determination of carcinoembryonic antigen in serum using inductively coupled plasma-mass spectrometry. *Analytica Chimica Acta*, 847, 10–15. <https://doi.org/10.1016/j.aca.2014.08.041>
- Dalmis, R., Birlik, I., Ak Azem, N. F., & Celik, E. (2020). Structurally colored silica photonic crystal coatings modified by Ce or Eu rare-earth dopants. *Colloids and Surfaces A: Physicochemical and Engineering Aspects*, 603(June 2020), 125138. <https://doi.org/10.1016/j.colsurfa.2020.125138>
- Danaei, M., Dehghankhold, M., Ataei, S., Hasanzadeh Davarani, F., Javanmard, R., Dokhani, A., Khorasani, S., & Mozafari, M. R. (2018). Impact of particle size and polydispersity index on the clinical applications of lipidic nanocarrier systems. *Pharmaceutics*, 10(2), 1–17. <https://doi.org/10.3390/pharmaceutics10020057>
- De Moraes, A., Silveira, G., Villis, P. C. M., Maroneze, C. M., Gushikem, Y., Pissetti, F. L., & Lucho, A. M. S. (2012). Gold nanoparticles on a thiol-functionalized silica network for ascorbic acid electrochemical detection in presence of dopamine and uric acid. *Journal of Solid State Electrochemistry*, 16(9), 2957–2966. <https://doi.org/10.1007/s10008-012-1701-z>
- del Valle, M. (2021). Sensors as green tools in analytical chemistry. *Current Opinion in Green and Sustainable Chemistry*, 31, 100501.

- <https://doi.org/10.1016/J.COGSC.2021.100501>
- Dundas, C. M., Demonte, D., & Park, S. (2013). Streptavidin-biotin technology: Improvements and innovations in chemical and biological applications. *Applied Microbiology and Biotechnology*, 97(21), 9343–9353. <https://doi.org/10.1007/s00253-013-5232-z>
- Fadzil, N. A. M., Rahim, M. H. A., & Maniam, G. P. (2018). Room temperature synthesis of ceria by the assisted of cationic surfactant and aging time. *Malaysian Journal of Analytical Sciences*, 22(3), 404–415. <https://doi.org/10.17576/mjas-2018-2203-05>
- Fazrin, E. I., Sari, A. K., Setiyono, R., Gaffar, S., Sofiatin, Y., Bahti, H. H., & Hartati, Y. W. (2022). The Selectivity and Stability of Epithelial Sodium Channel (ENaC) Aptamer as an Electrochemical Aptasensor. *Analytical & Bioanalytical Electrochemistry*, 14(7), 715–729.
- Firdaus, M. L., Madina, F. E., Sasti, Y. F., Elvia, R., Ishmah, S. N., Eddy, D. R., & Cid-Andres, A. P. (2020). Silica extraction from beach sand for dyes removal: Isotherms, kinetics and thermodynamics. *Rasayan Journal of Chemistry*, 13(1), 249–254. <https://doi.org/10.31788/RJC.2020.1315496>
- García-Rubio, D. L., de la Mora, M. B., Cerecedo, D., Saniger Blesa, J. M., & Villagrán-Muniz, M. (2020). An optical-based biosensor of the epithelial sodium channel as a tool for diagnosing hypertension. *Biosensors and Bioelectronics*, 157(March). <https://doi.org/10.1016/j.bios.2020.112151>
- Hartati, Y. W., Gaffar, S., Alfiani, D., Pratomo, U., Sofiatin, Y., & Subroto, T. (2020). A voltammetric immunosensor based on gold nanoparticle - Anti-ENaC bioconjugate for the detection of epithelial sodium channel (ENaC) protein as a biomarker of hypertension. *Sensing and Bio-Sensing Research*, 29(April). <https://doi.org/10.1016/j.sbsr.2020.100343>
- Hartati, Y. W., Komala, D. R., Hendrati, D., Gaffar, S., Hardianto, A., Sofiatin, Y., & Bahti, H. H. (2021). An aptasensor using ceria electrodeposited-screen-printed carbon electrode for detection of epithelial sodium channel protein as a hypertension biomarker. *Royal Society Open Science*, 8(2). <https://doi.org/10.1098/rsos.202040>
- Hartati, Y. W., Yusup, S. F., Fitrilawati, Wyantuti, S., Sofiatin, Y., & Gaffar, S. (2020). A voltammetric epithelial sodium channels immunosensor using screen-printed carbon electrode modified with reduced graphene oxide. *Current Chemistry Letters*, 9(4), 151–160. <https://doi.org/10.5267/j.ccl.2020.2.001>
- Hyre, D. E. (2006). Cooperative hydrogen bond interactions in the streptavidin-biotin system. *Protein Science*, 15(3), 459–467. <https://doi.org/10.1110/ps.051970306>
- Intartaglia, R., Bagga, K., Scotto, M., Diaspro, A., & Brandi, F. (2012). Luminescent silicon nanoparticles prepared by ultra short pulsed laser ablation in liquid for imaging applications. *Optical Materials Express*, 2(5), 510. <https://doi.org/10.1364/ome.2.000510>
- Ishmah, S. N., Permana, M. D., Firdaus, M. L., & Eddy, D. R. (2020). Extraction of Silica from Bengkulu Beach Sand using Alkali Fusion Method. *PENDIPA Journal of Science Education*, 4(2), 1–5. <https://doi.org/10.33369/pendipa.4.2.1-5>
- Ismail, S., Yusof, N. A., Abdullah, J., & Abd Rahman, S. F. (2020a). Development of Electrochemical Sensor Based on Silica/Gold Nanoparticles Modified Electrode for Detection of Arsenite. *IEEE Sensors Journal*, 20(7), 3406–3414. <https://doi.org/10.1109/JSEN.2019.2953799>
- Ismail, S., Yusof, N. A., Abdullah, J., & Abd Rahman, S. F. (2020b). Electrochemical detection of arsenite using a silica nanoparticles-modified screen-printed carbon electrode. *Materials*, 13(3168), 1–16. <https://doi.org/10.3390/ma13143168>
- Jalilpour, M., & Fathalilou, M. (2012). Effect of aging time and calcination temperature on the cerium oxide nanoparticles synthesis via reverse co-precipitation method. *International Journal of the Physical Sciences*, 7(6), 944–948. <https://doi.org/10.5897/ijps11.131>
- Jekel, C. F., Haftka, R. T., Venter, G., & Venter, M. P. (2018). Lack-of-fit Tests to Indicate Material Model Improvement or Experimental Data Noise Reduction. *January*. <https://doi.org/10.2514/6.2018-1664>
- Kalambate, P. K., Rao, Z., Dhanjai, Wu, J., Shen, Y., Boddula, R., & Huang, Y. (2020). Electrochemical (bio) sensors go green.

- Biosensors and Bioelectronics, 163, 112270. <https://doi.org/10.1016/J.BIOS.2020.112270>
- Khan, M. S., Dosoky, N. S., Berdiev, B. K., & Williams, J. D. (2016). Electrochemical impedance spectroscopy for black lipid membranes fused with channel protein supported on solid-state nanopore. *European Biophysics Journal*, 45(8), 843–852. <https://doi.org/10.1007/s00249-016-1156-8>
- Khan, M. S., Dosoky, N. S., Mustafa, G., Patel, D., Berdiev, B., & Williams, J. D. (2017). Electrophysiology of Epithelial Sodium Channel (ENaC) Embedded in Supported Lipid Bilayer Using a Single Nanopore Chip. *Langmuir*, 33(47), 13680–13688. <https://doi.org/10.1021/acs.langmuir.7b02404>
- Komala, D. R., Hardianto, A., Gaffar, S., & Hartati, Y. W. (2021). An epithelial sodium channel (ENaC)-specific aptamer determined through structure-based virtual screening for the development of hypertension early detection system. *Pharmaceutical Sciences*, 27(1), 67–75. <https://doi.org/10.34172/PS.2020.63>
- Li, J., Hao, Y., Li, H., Xia, M., Sun, X., & Wang, L. (2009). Direct synthesis of CeO<sub>2</sub>/SiO<sub>2</sub> mesostructured composite materials via sol-gel process. *Microporous and Mesoporous Materials*, 120(3), 421–425. <https://doi.org/10.1016/j.micromeso.2008.12.014>
- Ma, Q., Li, Y., & Su, X. (2015). Silica-nanobead-based sensors for analytical and bioanalytical applications. *Trends in Analytical Chemistry*, 74, 130–145. <https://doi.org/10.1016/j.trac.2015.06.006>
- Maharani, D. K., & Hidayah, R. (2015). PREPARATION AND CHARACTERIZATION OF CHITOSAN-ZnO/Al<sub>2</sub>O<sub>3</sub> COMPOSITE. *Molekul*, 10(3500), 9–18.
- Nguyen, H. T. T., Ohtani, M., & Kobiro, K. (2019). One-pot synthesis of SiO<sub>2</sub>-CeO<sub>2</sub> nanoparticle composites with enhanced heat tolerance. *Microporous and Mesoporous Materials*, 273, 35–40. <https://doi.org/10.1016/j.micromeso.2018.06.043>
- Perincek, O., & Colak, M. (2013). Use of Experimental Box-Behnken Design for the Estimation of Interactions Between Harmonic Currents Produced by Single Phase Loads. *International Journal of Engineering Research and Applications*, 3(2), 158–165.
- Phanichphant, S., Nakaruk, A., & Channei, D. (2016). Photocatalytic activity of the binary composite CeO<sub>2</sub>/SiO<sub>2</sub> for degradation of dye. *Applied Surface Science Journal*, 387, 214–220. <https://doi.org/10.1016/j.apsusc.2016.06.072>
- Pujar, M. S., Hunagund, S. M., Desai, V. R., Patil, S., & Sidarai, A. H. (2018). One-step synthesis and characterizations of cerium oxide nanoparticles in an ambient temperature via Co-precipitation method. *AIP Conference Proceedings*, 1942(April), 1–6. <https://doi.org/10.1063/1.5028657>
- Radojković, M., Zeković, Z., Jokić, S., & Vidović, S. (2012). Determination of optimal extraction parameters of mulberry leaves using response surface methodology (RSM). *Romanian Biotechnological Letters*, 17(3), 7295–7308.
- Reus-Chavarría, E., Martínez-Vieyra, I., Salinas-Nolasco, C., Chávez-Piña, A. E., Méndez-Méndez, J. V., López-Villegas, E. O., Sosa-Peinado, A., & Cerecedo, D. (2019). Enhanced expression of the Epithelial Sodium Channel in neutrophils from hypertensive patients. *Biochimica Biophysica Acta - Biomembranes*, 1861(2), 387–402. <https://doi.org/10.1016/j.bbamem.2018.11.003>
- Sakamoto, S., Putalun, W., Vimolmangkang, S., Phoolcharoen, W., Shoyama, Y., Tanaka, H., & Morimoto, S. (2018). Enzyme-linked immunosorbent assay for the quantitative/qualitative analysis of plant secondary metabolites. *Journal of Natural Medicines*, 72(1), 32–42. <https://doi.org/10.1007/s11418-017-1144-z>
- Sari, A. K., Hartati, Y. W., Gaffar, S., Anshori, I., Hidayat, D., & Wiraswati, H. L. (2022). The optimization of an electrochemical aptasensor to detect RBD protein S SARS-CoV-2 as a biomarker of COVID-19 using screen-printed carbon electrode/AuNP. *Journal of Electrochemical Science and Engineering*, 12(1), 219–235. <https://doi.org/10.5599/jese.1206>
- Scholz, F. (2010). Guide to experiments and applications: Pulse Voltammetry. In *Electroanalytical Methods*. Springer-Verlag Berlin Heidelberg

- <https://doi.org/10.1007/978-3-642-02915-8>  
Sedlak, S. M., Schendel, L. C., Gaub, H. E., & Bernardi, R. C. (2020). Streptavidin/biotin: Tethering geometry defines unbinding mechanics. *Science Advances*, 6(13), 1–11. <https://doi.org/10.1126/sciadv.aay5999>
- Siangproh, W., Dungchai, W., Rattanarat, P., & Chailapakul, O. (2011). Nanoparticle-based electrochemical detection in conventional and miniaturized systems and their bioanalytical applications: A review. *Analytica Chimica Acta*, 690(1), 10–25. <https://doi.org/10.1016/j.aca.2011.01.054>
- Sofiatin, Y., & MA Roesli, R. (2018). Detection of Urinary Epithelial Sodium Channel (ENaC) Protein. *American Journal of Clinical Medicine Research*, 6(2), 20–23. <https://doi.org/10.12691/ajcmr-6-2-1>
- Tan, H., Ma, L., Guo, T., Zhou, H., Chen, L., Zhang, Y., Dai, H., & Yu, Y. (2019). A novel fluorescence aptasensor based on mesoporous silica nanoparticles for selective and sensitive detection of aflatoxin B 1. *Analytica Chimica Acta*, 1068(2), 87–95. <https://doi.org/10.1016/j.aca.2019.04.014>
- Vert, M., Doi, Y., Hellwich, K., Hess, M., Hodge, P., Kubisa, P., Rinaudo, M., & Schué, F. (2012). Terminology for biorelated polymers and applications ( IUPAC Recommendations 2012 )\*. *Pure and Applied Chemistry*, 84(2), 377–410.
- Walcarius, A. (2018). Silica-based electrochemical sensors and biosensors: Recent trends. *Current Opinion in Electrochemistry*, 10, 88–97. <https://doi.org/10.1016/j.coelec.2018.03.017>
- Wang, J., Guo, J., Zhang, J., Zhang, W., & Zhang, Y. (2017). RNA aptamer-based electrochemical aptasensor for C-reactive protein detection using functionalized silica microspheres as immunoprobos. *Biosensors and Bioelectronics*, 95, 100–105. <https://doi.org/10.1016/j.bios.2017.04.014>
- Wyantuti, S., Harahap, F. W., Hartati, Y. W., & Firdaus, M. L. (2021). Application of Plackett-Burman and Box-Behnken experimental designs in differential voltammetry for determining Gadolinium concentration. *Journal of Physics: Conference Series*, 1731(1). <https://doi.org/10.1088/1742-6596/1731/1/012017>
- Xu, W., Huang, Y., Li, L., Sun, Z., Shen, Y., Xing, J., Li, M., Su, D., & Liang, X. (2016). Hyperuricemia induces hypertension through activation of renal epithelial sodium channel (ENaC). *Metabolism: Clinical and Experimental*, 65(3), 73–83. <https://doi.org/10.1016/j.metabol.2015.10.026>
- Xunwen, S., Liquan, Z., Weiping, L., Huicong, L., & Hui, Y. (2020). The synthesis of monodispersed M-CeO<sub>2</sub>/SiO<sub>2</sub> nanoparticles and formation of UV absorption coatings with them. *Royal Society of Chemistry*, 10, 4554–4560. <https://doi.org/10.1039/c9ra08975f>
- Zakiyyah, S. N., Eddy, D. R., Firdaus, M. L., Subroto, T., & Hartati, Y. W. (2022). Screen-printed carbon electrode/natural silica-ceria nanocomposite for electrochemical aptasensor application. *Journal of Electrochemical Science and Engineering*, 00(0), 1–18. <https://doi.org/10.5599/jese.1455>